

# **Studying Conformational Dynamics of Amyloidogenic Proteins using Fluorescence Spectroscopy**

**Anubhuti Singh**

*A dissertation submitted for the partial fulfilment of*

*BS-MS Dual Degree in Science*



**Department of Chemical Sciences**

**Indian Institute of science Education and Research (IISER) Mohali**

**April 2015**



## **Certificate of Examination**

This is to certify that dissertation titled “Studying conformational dynamics of amyloidogenic proteins using fluorescence spectroscopy” submitted by Ms. Anubhuti Singh (MS10097) for the partial fulfilment of the BS-MS dual degree programme of the Institute, has been examined by thesis committee duly appointed by institute. Committee finds the work done by candidate satisfactory and recommends that the report be accepted.

Dr. Santanu Kumar Paul

Dr. Sabyasachi Rakshit

Dr. Samrat Mukhopadhyay

(Supervisor)



## **Declaration**

The work presented in the dissertation has been carried out by me under the supervision of Dr. Samrat Mukhopadhyay at the Department of Chemical Sciences, Indian Institute of Science Education and Research (IISER) Mohali.

This work has not been submitted in part or full for a degree, a diploma, or a fellowship to any other university or institute.

Whenever contributions of others are involved, every effort is made to indicate this clearly, with due acknowledgement of collaborative research and discussions. This thesis is a bona fide record of original work done by me and all sources listed within have been detailed in bibliography.

Date

Anubhuti Singh

In my capacity as the supervisor of the candidate's thesis work, I certified that the above statements by the candidate are true to the best of my knowledge.

Dr. Samrat Mukhopadhyay

(Supervisor)



## Acknowledgement

Foremost, I would like to express my sincere gratitude to my master's thesis supervisor Dr. Samrat Mukhopadhyay for his continuous support, patience, motivation and enthusiasm. It was under his tutelage I got interested in the field of chemical biology. I appreciate his vast knowledge and skill in many areas and his assistance in writing reports (i.e, graduate applications and this thesis). Discussions held with him, helped me enormously in diversifying my knowledge. Whenever experiments did not work and I used to get frustrated, his saying "You just have to collect your acts together, I know you can do it better" kept me motivated throughout my project. His mentorship has helped me to grow as a young scientist. I doubt that I will ever be able to convey my appreciation fully, but I owe him my eternal gratitude.

Besides my advisor, I would like to thank the rest of my thesis committee: Dr. Santanu Kumar Paul, Dr. Sabyasachi Rakshit for their encouragement and insightful comments.

I would like to thank Karishma Bhasne for her advices and guidance throughout my tenure. She helped me in  $\alpha$ -synuclein project and has taught me everything related to this protein. She has guided me in designing the experiments and helped me in acquiring the time-resolved anisotropy data. Her immense love and care always made me smile during the hardest phase in the lab actually chocolates are the one who made me smile.

I would like to thank Dominic Narang for his immense help throughout the project. He is the senior most and busiest person in the lab, then to he taught me the basics of molecular biology. He supported me throughout the project especially in the cloning and labelling step. Stimulating discussions with him has brought a new insight in me for science. Apart from that, he was the support pillar for me in the lab. I look up to him for any help and advice. He has always taken care of me as a little girl.

I thank my other labmates: Mily, Vijit, Shruti, Hema, Priyanka, Nilanjana, Simarbeer and other past members of Mukhopadhyay lab for their valuable suggestions and support, which helped me in shaping the thesis in a better way. I would also thank them for all the fun in lab, sleepless nights when we were working together and for discussions and exchanges of knowledge, skills, which helped me in enriching the scientific temper.





I am also thankful to Department of Science and Technology (DST), Govt.of India, for the INSPIRE Fellowship. I am grateful to Indian Institute of Science Education and Research (IISER) Mohali, for providing all the facilities for my research work.

A friend in need is a friend indeed. Life will be so boring without friends. I have enjoyed my most of the time with Priyanka, Meenakshi, Ashima, TJ, Haseeb, Promit, Rupali, Zeeshan, Vanika, Shady. Late night walks and chatting with them has always makes me relax after a long busy day in lab.

Last but not the least; I would like to thank my family for their love, support and encouragement. I would also like to thank my Uncle, for his love, care and usual visits that helped me in avoiding home sickness.



## List of Figures

**Figure 1.**(a) Sequence of  $\alpha$ -synuclein showing distribution of charged amino acids. Residues underlined were replaced by cysteine (b) SDS-PAGE showing fractions of pure  $\alpha$ -synuclein (c) Different regions of  $\alpha$ -synuclein with mutant positions highlighted in yellow.

**Figure 2.**(a) CD spectra of wild-type (WT) (Pink) and cysteine mutant (Green) and change in secondary structure from random coil (Green: Native) to  $\alpha$ -helix with SUVs (Blue) and LUVs (Red) (b) Schematic diagram to show the transition from disorder form to helical state.

**Figure 3.**Picosecond time-resolved fluorescence anisotropy decays  $r(t)$  in the absence and presence of POPG SUVs of A90C. The solid line (Red) is the bi-exponential fit and tri-exponential fit respectively.

**Figure 4.**(a) Sequence of  $\beta_2m$  (b) Ribbon diagram of  $\beta_2m$  generating using PyMol (Delano Scientific LLC, CA) from the Protein Data Bank (PDB ID: 1LDS). (c) Fluorescence emission spectra of  $\beta_2m$  (W60) as function of increasing concentration of GdmCl (d) intensity ratios at 330nm and 360nm of  $\beta_2m$  (W60) as a function of increasing concentration of GdmCl.

**Figure 5.**(a) Structure of  $\beta_2m$ , the location of W60 and cysteine is shown along with the TNB. The sole thiol moiety was labelled with TNB that quenches the fluorescence of Trp in a distance-dependent manner. The TNB-labelled protein named as W60 NTC-TNB. Structure was drawn from PDB file by using the program PyMOL. (b) Fluorescence emission spectra of unlabelled and TNB-labelled protein in native condition. (c) Fluorescence emission spectra of unlabelled and TNB-labelled protein in 4 M GdmCl.

**Figure 6.**FRET efficiency is plotted against GdmCl concentration. The data for unlabelled and TNB-labelled protein is collected at the emission wavelength of 350 nm after excitation at 295 nm. The red continues line through the data represent the Boltzman fits to a two-state native  $\leftrightarrow$  unfolded model.

## List of table

**Table1.** IAEDANS fluorescence lifetime and rotational correlation time for single-Cys mutant of  $\alpha$ -synuclein (A90C) in the absence and presence of lipid membranes.

# Contents

<b>List of figure.....</b>	<b>i</b>
<b>List of table.....</b>	<b>ii</b>
<b>Abstract.....</b>	<b>v</b>
<b>Chapter 1:</b>	
<b>Introduction.....</b>	<b>1</b>
1. Basic Theory.....	1
2. Experimental Methods.....	3
2.1 Materials.....	3
2.2 Protein expression and purification.....	3
2.2.1 $\alpha$ -synuclein.....	3
2.2.2 $\beta_2$ -microglobulin.....	4
2.3 Preparation of protein sample.....	5
2.3.1 $\alpha$ -synuclein.....	5
2.3.2 $\beta_2$ -microglobulin.....	5
2.4 Fluorescence labelling of proteins.....	6
2.4.1 $\alpha$ -synuclein with IAEDANS.....	6
2.4.2 $\beta_2$ m (W60-N Terminal cysteine) with DTNB.....	7
2.5 Lipid vesicle preparation.....	7
2.5.1 Preparation of Small Unilamellar vesicles (SUVs).....	8
2.5.2 Preparation of Large Unilamellar vesicles (LUVs).....	8
2.6 Circular Dichroism (CD) experiments.....	8
2.7 Steady-state fluorescence measurements.....	8
2.7.1 FRET (Fluorescence resonance energy transfer).....	9
2.8 Time-resolved fluorescence measurements.....	9
2.8.1 AEDANS fluorescence intensity decay.....	9
2.8.2 AEDANS fluorescence anisotropy decay.....	10
<b>Chapter 2: Results and Discussion.....</b>	<b>11</b>
1. Results.....	11

1.1 Membrane-induced $\alpha$ -helical structure conformation of $\alpha$ -synuclein.....	11
1.2 Site-specific conformational dynamics of membrane-bound $\alpha$ -synuclein.....	12
1.3 GdmCl-induced unfolding of Human $\beta_2$ -microglobulin.....	14
1.4 Thionitrobenzoate (TNB) quenches the fluorescence of tryptophan in a distance-dependent manner upon unfolding.....	15
2. Conclusion and Future outlooks.....	17
<b>Bibliography.....</b>	<b>18</b>

# STUDYING CONFORMATIONAL DYNAMICS OF AMYLOIDOGENIC PROTEINS USING FLUORESCENCE SPECTROSCOPY

**Anubhuti Singh**

Department of Chemical Sciences

Indian Institute of science Education and Research (IISER) Mohali

MS Thesis Supervisor: Dr. Samrat Mukhopadhyay

## **Abstract:**

Protein misfolding leading to amyloid aggregation has attracted considerable interest due to its connection to a range of neurological disorders. It is important to characterize the conformational behaviour of the early oligomeric state of amyloidogenic proteins that serve as precursor to toxic amyloid in order to understand the molecular mechanism of amyloidogenesis. Fluorescence Spectroscopy has been an invaluable tool for the study of biomolecular systems. It is one of the most powerful methods to study protein folding, dynamics, assembly and interactions. In the structural and dynamical studies of proteins, fluorescence spectroscopy is well suited because of its high experimental sensitivity and selectivity to a protein's environment. The present work comprises the study of two amyloidogenic proteins, namely  $\alpha$ -synuclein and  $\beta_2$ -microglobulin ( $\beta_2m$ ), aggregation of which are involved in Parkinson's disease and dialysis-related amyloidosis, respectively.  $\alpha$ -synuclein is an intrinsically disordered protein that is preferentially expressed in presynaptic nerve terminals. It undergoes a large-scale conformational rearrangement upon binding to synaptic vesicle membranes. In order to obtain the structural insights into the membrane-bound  $\alpha$ -synuclein in the residue specific manner, we incorporated single cysteine (Cys) at various positions along the sequence. These Cys mutants were labelled with an extrinsic fluorophore, IAEDANS and were used as site-specific fluorescence marker to characterize the dynamical aspects of  $\alpha$ -synuclein. On the other hand,  $\beta_2m$  has a classical  $\beta$ -sandwich fold comprising seven antiparallel  $\beta$ -strands and is a component of the major histocompatibility complex class I. Here we have focused on conformational states of  $\beta_2m$  that would be involved in unfolding process as an intermediate state using a host of fluorescence spectroscopic tools. These tools allowed us to monitor the conformational changes of  $\beta_2m$  during its unfolding process.

# Chapter 1

## Introduction

### 1. Basic Theory:

Protein misfolding, aggregation, and amyloid fibril formation are associated with a number of human disorders that include Alzheimer's, Parkinson's, Huntington's, and prion diseases as well as type II diabetes and dialysis-related amyloidosis.<sup>1-4</sup> Understanding the molecular mechanism of amyloid formation would represent an important step in elucidating the conformational behaviour of the early oligomeric state of amyloidogenic proteins. Various studies on amyloidogenic proteins have indicated that the presence of intrinsically disordered or partially unfolded structure in the polypeptide chains plays a pivotal role in initiating the process of amyloid assembly.<sup>5-11</sup> There is an emerging consensus that the conformational properties of amyloidogenic disordered polypeptides are in sharp contrast to those of the prototypal denatured state of proteins found in high concentration of chemical denaturant. The mechanism of amyloidogenesis for intrinsically disordered proteins (IDPs) and natively folded proteins are in contrast. In case of IDPs, disorderedness is a necessary condition for aggregation. It has been shown that a very small change in the environment of such proteins often might cause their partial folding and aggregation.<sup>12</sup> Whereas, in case of natively structured proteins, partial unfolding is believed to be a prerequisite for the proteins' assembly into amyloid fibrils.<sup>13</sup> Thus, to understand the molecular mechanism of amyloidosis, it is necessary to find factors that induce partial unfolding in natively structured proteins as well as partial folding in IDPs and subsequent amyloid fibril formation.

Present work involves the study of structural and conformational dynamics of two amyloidogenic proteins, namely human  $\alpha$ -synuclein and human  $\beta_2$ -microglobulin ( $\beta_2m$ ), aggregation of which are involved in Parkinson's disease and dialysis-related amyloidosis, respectively. Alpha-synuclein ( $\alpha$ -synuclein) is a small (14kDa, 140 amino acids), highly acidic, intrinsically unstructured protein that is expressed predominantly in the human brain and concentrated in presynaptic nerve terminals. Structurally,  $\alpha$ -synuclein sequence is divided into three distinct regions (Figure 1(a)): N-terminal (1-60 amino acid) which has an affinity to bind to the membranes<sup>14</sup>, central region (61-95 amino acid) known as NAC region (non-amyloid component of Alzheimer disease



amyloid) which initiates the aggregation<sup>15</sup> and the third region C-terminal (96-140 amino acid) is highly negatively charged and it facilitates the binding of calcium and other ions.<sup>16</sup> The exact function of  $\alpha$ -synuclein protein is poorly understood, though, there are few proposed functions known such as synaptic transmission<sup>17</sup>, synaptic vesicle localization<sup>18</sup>, and maintenance of neuronal plasticity<sup>19</sup> etc. Furthermore, the N-terminal domain of  $\alpha$ -synuclein includes 7 imperfect 11-residue repeats, each containing a variant of the consensus 6-residue sequence KTKEGV, which are similar to repeats found in the exchangeable apo-lipoproteins and are consistent with a class A2 amphipathic  $\alpha$ -helices<sup>20</sup> suggesting a lipid-binding activity for N-terminal domain.  $\alpha$ -synuclein was shown to associate with synaptic vesicles<sup>21</sup> and to bind to synthetic containing negatively-charged phospholipids.<sup>22</sup> Many biophysical experiments have been performed to understand the interaction between membrane and  $\alpha$ -synuclein, the results showed that  $\alpha$ -synuclein undergoes a conformational change from random coil to  $\alpha$ -helical structure.<sup>23</sup> But the in-depth residue-specific information of the membrane bound  $\alpha$ -synuclein is still remains elusive. Therefore, in order to understand conformational transitions of  $\alpha$ -synuclein in residue specific manner, we have employed time-resolved fluorescence anisotropy of an environment-sensitive fluorophore, 5-(((2-iodoacetyl) amino) ethyl) amino) naphthalene-1-sulfonic acid (IAEDANS), attached to specific locations in the protein, as a readout. Single cysteine mutant of  $\alpha$ -synuclein (A90C) was used for studies. The protein was labelled with IAEDANS, a thiol-labelling fluorescence probe. The site-specific fluorescence anisotropy decay of labelled protein was monitored to probe the conformational dynamics of  $\alpha$ -synuclein upon binding to membranes. The results show that the NAC region (Cys 90) is highly structured as indicated by high anisotropy and also showed different degree of structural organization.

$\beta_2$ -microglobulin ( $\beta_2$ m) is a light chain of the class I major histocompatibility complex (MHC), which is non-covalently attached to the  $\alpha$ -chain of the MHC I molecule. Amyloid fibril formation of  $\beta_2$ m is implicated in dialysis-related amyloidosis, a disease reported among those patients who receive prolonged hemodialysis.<sup>24</sup> It is a 99 amino acid residue protein, comprising seven  $\beta$ -strands with a disulfide bond between Cys25 and Cys80, and contains two tryptophan residues at positions 60 and 95 of the polypeptide chain (Figure 4).<sup>25, 26</sup> The tryptophan residue at position 60 is largely exposed, whereas that at position 95 is partially buried.<sup>26</sup> Previous studies have shown

that the transition of  $\beta_2m$  from soluble state to insoluble aggregates can be triggered at low pH with accumulation of distinct intermediate states.<sup>27, 28</sup> A population of a partially unfolded intermediate, possessing the characteristics of a molten globule-like state, builds up at pH 3.6, as also supported by nuclear magnetic resonance (NMR) studies.<sup>27</sup> In the present investigation, we directed our efforts to understand the mechanism of GdmCl-induced unfolding of  $\beta_2m$  using a diverse array of fluorescence spectroscopic tools that allow us to monitor conformational dynamics and chain dimension in the low protein concentration regime. Our fluorescence studies provide an important dynamic signature of an intermediate state of  $\beta_2m$  during the unfolding process that is different from that of the native state and canonical unfolded states of proteins.

## **2. Experimental Section:**

### **2.1 Materials:**

LB (Luria Broth mixture powder), agar powder, Tris, Glycine, SDS (sodium dodecyl sulphate), NaCl (sodium chloride) were purchased from Hi-Media. EDTA (ethylenediaminetetraacetic acid), protease inhibitor cocktail, HEPES (4-(2-hydroxyethyl) piperazine-1-ethanesulfonic acid), DTT (dithiothreitol), Dimethylsulfoxide (DMSO) were purchased from Sigma and used as received. Ampicillin, chloramphenicol and IPTG (isopropyl beta-D-1-thiogalactopyranoside) were purchased from Goldbio.Com. HCL (hydrochloric acid), CaCl<sub>2</sub> (calcium chloride), ethanol, glacial acetic acid and ammonium sulphate were purchased from Merck. Q (quaternary ammonium) sepharose fast flow resin was purchased from GE Healthcare and streptomycin sulphate was purchased from CDH and used as received. Chloroform solutions of POPG (1-palmitoyl-2-oleoyl-sn-glycero-3-phospho (1'-rac-glycerol)) were purchased from Avanti Polar Lipids. Guanidium hydrochloride (GdmCl), 5-((((2-(iodoacetyl) amino) ethyl) amino) naphthalene-1-sulfonic acid) (IAEDANS) and dithionitrobenzionate (DTNB) were purchased from Sigma.

### **2.2 Protein Expression and Purification**

**2.2.1  $\alpha$ -synuclein:** Cysteine mutants of  $\alpha$ -synuclein were purified using a reported protocol. The pT7-7 plasmid with  $\alpha$ -synuclein gene was kindly provided by Prof. Vinod

Subramaniam from the University of Twente, The Netherlands. It was transformed in BL21 (DE3) strain of *Escherichia coli*. Briefly, 1% of the overnight grown culture (containing 100 µg/ml) ampicillin and (35 µg/ml) chloramphenicol of BL21 (DE3) was transformed into fresh media (containing 100 µg/ml ampicillin) and when O.D at 600nm reached to 0.6 – 0.8, the cells were induced with 800 µM IPTG for 4 hours. To obtain the cell pellet, culture was centrifuged at 4,000rpm for 30 min at 4 °C. Pellet was resuspended in lysis buffer (50 mM Tris, 150 mM NaCl, 10 mM EDTA, pH 8.0 containing 50 µL protease inhibitor cocktail) and stored at -80 °C till further use. The lysed cells were boiled at 95 °C for 30 min followed by centrifugation at 12,000 rotation per minute (rpm) for 30 min at 4 °C. The supernatant was collected and thoroughly mixed with 136 µL/mL of 10% streptomycin sulphate and 228 µL/mL of glacial acetic acid followed by centrifugation at 12,000 rpm for 30 min at 4 °C. To the clear supernatant, equal volume of saturated ammonium sulphate was added and kept at 4 °C with an intermittent mixing for an hour. The precipitated protein, separated by centrifugation at 12,000 rpm for 30 min at 4 °C was suspended in equal volume of 100 mM ammonium acetate and ethanol followed by centrifugation at 4,000 rpm for 10 min at 4 °C. Finally, the pellet was washed with absolute ethanol and dried at room temperature, until ethanol evaporated. The pellet was suspended in equilibrating buffer (10 mM Tris, pH 7.4) and further purified by FPLC (fast performance liquid chromatography) on a Q Sepharose and the protein was eluted at ~ 300 mM NaCl. The purity of the collected fractions was assessed by SDS- PAGE (SDS- polyacrylamide gel electrophoresis) (Figure 1(b)). The pure fractions were dialyzed in a dialysis duffer (10 mM HEPES, 50 mM NaCl, pH 7.4) and stored at -80 °C.

### **2.2.2 Human $\beta_2$ -microglobulin ( $\beta_2m$ ):**

pET-23a plasmid harbouring mutant of human  $\beta_2m$  gene (W60 & W60 N terminal Cysteine) was expressed in *Escherichia coli* BL21 DE3-lysogen cells. Briefly, 1% of the overnight grown culture (containing 100 µg/ml ampicillin and 35 µg/ml chloramphenicol) of BL21 (DE3) was transformed into fresh media (containing 100 µg/ml ampicillin) and when O.D at 600nm reached to 0.6 – 0.8, the cells were induced with 1 mM IPTG for 8-10 hours. To obtain the cell pellet, culture was centrifuged at 4,000 rpm for 30 min at 4 °C. Pellet was resuspended in lysis buffer (10 mM Tris, 1 mM EDTA, pH 8.0). The lysed cells were sonicated (Amplitude= 20, pulse on time= 10sec for 30 min) followed by

centrifugation at 12,000 rpm for 30 min at 4 °C and inclusion bodies were stored at -80 °C for further use. The inclusion bodies were resuspended in 8 M urea and kept in 4 °C overnight. Insoluble material was removed by centrifugation and the solubilized  $\beta_2m$  was then refolded by dialysis into dialysis buffer (10 mM Tris, 1 mM EDTA, pH 8.0) at room temperature. Dialysed protein was purified on an anion exchanger (Q-Sepharose from GE) column, by performing fast flow protein liquid chromatography (FFPLC). Fractions showing single peak were separately pooled and further purified using a Superdex-75 column (GE). Stock of solution of purified recombinant protein was stored at 4 °C.

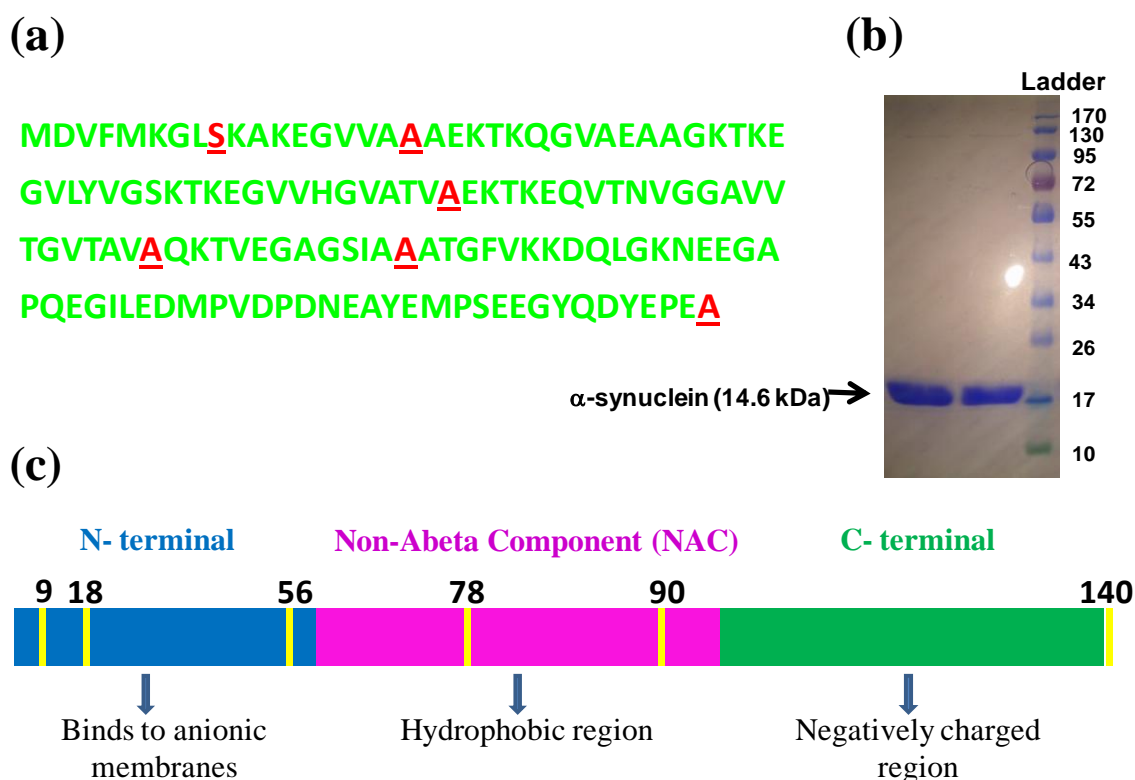


**Figure 1.** (a) Sequence of  $\alpha$ -synuclein showing distribution of charged amino acids. Residues underlined were replaced by cysteine (b) SDS-PAGE showing fractions of pure  $\alpha$ -synuclein (c) Different regions of  $\alpha$ -synuclein with mutant positions highlighted in yellow.

## 2.3 Preparation of protein sample:

### 2.3.1 $\alpha$ -synuclein:

Prior to every experiment the single cysteine mutants of  $\alpha$ -synuclein were passed through 50 kDa molecular weight cut off (MWCO) Amicon filter (purchased from Milipore) and concentrated using 3 kDa MWCO Amicon. The concentration of protein

was estimated by measuring absorbance using UV-Vis spectrophotometer (Chirascan, Applied photophysics). The concentration of all the mutants was determined using  $E_{275} = 10,810 \text{ M}^{-1} \text{ cm}^{-1}$ . The measurements were carried out using 1 mm path length cuvette with a scan range of 260-300nm and a scan rate of 1 nm/s. The final spectra averaged over 2 scans and buffer subtracted. The purified proteins were stored at  $-80 \text{ }^{\circ}\text{C}$ .

### **2.3. $\beta_2$ -microglobulin:**

Prior to every experiment the single tryptophan and N-terminal cysteine mutant of  $\beta_2\text{m}$  were concentrated using 3 kDa molecular weight cut off (MWCO) Amicon filter (purchased from Milipore). The concentrations of proteins were estimated by measuring tryptophan absorbance using UV-Vis spectrophotometer (Chirascan, Applied photophysics). The concentration of all the mutants was determined using  $E_{280} = 14,565 \text{ M}^{-1} \text{ cm}^{-1}$ . The measurements were carried out using 1mm path length cuvette with a scan range of 240-350 nm and a scan rate of 1 nm/s. The final spectra averaged over 3 scans and buffer subtracted. The purified proteins were stored at  $-80 \text{ }^{\circ}\text{C}$ .

For unfolding experiments, protein was incubated in different concentrations of GdmCl ranging from zero to 4 M for 12 hour, and the equilibrium fluorescence signals were measured.

### **2.4 Fluorescence labelling of proteins:**

#### **2.4.1 $\alpha$ -synuclein with IAEDANS:**

The labelling of the free thiol group in denatured  $\alpha$ -synuclein was carried out in 10 mM HEPES buffer and 50mM NaCl, pH 7.4. Initially, 50  $\mu\text{M}$  of  $\alpha$ -synuclein was prepared in 6 M GdmCl kept on spinning rotor for 2 hour at 10 rpm at  $25 \text{ }^{\circ}\text{C}$ . Approximately 30 equivalents of IAEDANS, dissolved in dry DMSO, were added into the denatured and reduced  $\alpha$ -synuclein and the reaction mixture was kept on rotor spin for 3 hour at room temperature. After the labelling reaction was complete, the labelled protein was dialyzed in a dialysis buffer (10mM HEPES, 50mM NaCl, pH 7.4) overnight and then concentrated using 3 kDa MWCO Amicon, whereby the free, unreacted dye was removed. Protein concentration was checked by measuring the absorbance at both 280 and 337 nm. The concentration of the labelled protein was determined by the subtracting

the absorption contribution of AEDANS at 280 nm. The molar extinction coefficients of IAEDANS at 280 nm and 337 nm are  $12800 \text{ M}^{-1} \text{ cm}^{-1}$  and  $6100 \text{ M}^{-1} \text{ cm}^{-1}$ , respectively.

#### **2.4.2 $\beta_2\text{m}$ (W60-N Terminal cysteine) with DTNB:**

The labelling of the free thiol group in denatured  $\beta_2\text{m}$  was carried out in 6M GdmCl and 20 mM phosphate buffer, pH 7. Initially, 500  $\mu\text{M}$  of  $\beta_2\text{m}$  was prepared in 6 M GdmCl to which an aqueous solution of 2 mM DTT was added. The resulting solution was kept on spinning rotor for 2 hour at 10 rpm at 37 °C and then in 4 degree for 3 hour. PD-10 de-salting column was used to refold the protein and to remove DTT. Just after removal of DTT, protein was again refolded using PD-10 in 6M GdmCl and labelled with approximately 100 equivalents of DTNB, dissolved in 6 M GdmCl. The reaction mixture was again kept on rotor spin for 3 hour at room temperature. After the labelling reaction was complete, the labelled protein was dialyzed into a dialysis buffer (10 mM Tris, 1 mM EDTA, pH 8.0) overnight and then concentrated using 3 kDa MWCO Amicon. PD-10 column was used to remove the free dye. Protein concentration was checked by measuring the absorbance at both 280 and 325 nm. The concentration of the labelled protein was determined by the subtracting the absorption contribution of TNB at 280 nm.

#### **2.5 Lipid vesicle preparation:**

Liposome's were made from anionic POPG using a reported protocol. Briefly, appropriate amount of the respective chloroform solution was taken in around bottom flask and purged with a gentle stream of nitrogen for 1 hr followed by vacuum desiccation for 2 hours to ensure complete removal of the residual organic solvent. The dried lipid film was hydrated in DPBS (Dulbecco's phosphate buffer saline: 2.67 mM KCl, 1.47 mM  $\text{KH}_2\text{PO}_4$ , 138 mM NaCl and 8.06 mM  $\text{Na}_2\text{HPO}_4$ , pH 7.4) buffer with intermittent vortexing for an hour to a final lipid concentration of 10 mM. This resulted in a turbid solution having MLVs (multilamellar vesicles). The MLVs were subjected to freeze-thaw cycles, alternating between liquid nitrogen and water bath (preset at 42 °C) for one minute.

### **2.5.1 Preparation of Small Unilamellar vesicles (SUVs):**

The above MLVs were then sonicated for an hour at 40 °C using 37 Hz pulse rate to obtain SUVs. The size of the SUVs (30 nm ± 10 nm) was confirmed by DAWN 8 Helios MALS system (Wyatt Technology).

### **2.5.2 Preparation of Large Unilamellar vesicles (LUVs):**

The above MLVs were subjected to extrusion method in order to prepare LUVs (Mini Extruder, Avanti Polar Lipids). The size of the LUVs (100 nm ± 10 nm) was confirmed by DAWN 8 Helios MALS system (Wyatt Technology).

### **2.6 Circular Dichroism (CD) experiments:**

The CD spectra were collected on Chirascan CD spectrometer (Applied Photophysics, UK) using a 1 mm path length quartz cuvette at room temperature. The concentrations of mutants of  $\alpha$ -synuclein and  $\beta_2m$  were fixed as 20  $\mu$ M.  $\alpha$ -synuclein CD spectra in the absence and presence of POPG (1 mM) in DPBS buffer were collected with a scan range of 1 nm/s and averaged over 3 scans. The scan range was fixed from 200 nm to 260 nm. All the spectra were buffer subtracted and smoothed using Chirascan 'ProData viewer' software provided with the instrument.

### **2.7 Steady-state fluorescence measurements:**

All steady-state fluorescence measurements were carried out on HORIBA Scientific Fluoromax-4 spectrofluorimeter. The steady-state anisotropy is given by:

$$r_{ss} = (I_{\parallel} - GI_{\perp}) / (I_{\parallel} + 2GI_{\perp}) \quad (1)$$

$r_{ss}$  was obtained from the parallel ( $I_{\parallel}$ ) and perpendicular ( $I_{\perp}$ ) intensity components with G-factor correction. For  $\alpha$ -synuclein, the final concentration of protein and lipids were 50  $\mu$ M and 2 mM, respectively in all experiments. For AEDANS fluorescence intensity measurements,  $\lambda_{ex}$  and  $\lambda_{em}$  were set to 295 nm (bandpass 1.0 nm) and 350 nm (bandpass 5.0 nm), respectively. The path length of the cuvette was 2 mm. Fluorescence intensity were recorded with integration time of 3 s. AEDANS fluorescence anisotropy was measured by setting  $\lambda_{ex}$  and  $\lambda_{em}$  to 295 nm (bandpass 1.0 nm) and 350 nm (bandpass 5.0 nm), respectively. Integration time of 3 s was used to obtain a satisfactory signal-to-noise ratio.

For  $\beta_2m$ , the final concentration of protein was 20  $\mu M$  in all experiments. For Trp fluorescence intensity,  $\lambda_{ex}$  and  $\lambda_{em}$  were set to 295 nm (bandpass 0.8 nm) and 350 nm (bandpass 3.0 nm), respectively. Integration time of 1 s was used to obtain a satisfactory signal-to-noise ratio.

### **2.7.1 FRET (Fluorescence resonance energy transfer):**

For fluorescence resonance energy transfer (Trp  $\rightarrow$  TNB) measurements, the concentration of  $\beta_2m$  mutant (W60 N-terminal cysteine) was kept constant in increasing concentration of GdmCl, pH 7.0, as 20  $\mu M$ . A cuvette (from Hellma) of path length 10 mm x 2 mm was used for the measurements. The tryptophan (Trp) decay in the absence and presence of labelled protein were collected and analyzed. The FRET efficiencies (E) were estimated from the fluorescence intensity of Trp in the absence ( $F_D$ ) and in the presence of acceptor ( $F_{DA}$ ) using following relationship.

$$E = 1 - (F_{DA} / F_D) \quad (2)$$

### **2.8 Time-resolved fluorescence measurements:**

The time-resolved fluorescence decays of the samples (in the absence and presence of cysteine variants labelled with IAEDANS or lipids) were collected using a time correlated single-photon-counting (TCSPC) setup (Fluorocube, Horiba Jobin Yvon, NJ). 375 nm LD (Laser Diode) was used as excitation source having repetition rate of 1 MHz. All the decays were collected at magic angle (54.7) with 12 nm bandpass and a PhotoMultiplier Tube (PMT) (Hamamatsu Corp) was used as detector. An aqueous solution of 2 % Ludox was used to collect the instrument response function (~ 200 ps). In order to obtain a good signal-to-noise ratio, 10,000 counts were collected at the peak. All the experiments were carried out at room temperature.

#### **2.8.1 AEDANS fluorescence intensity decay:**

For all the life time measurements, the concentration of  $\alpha$ -synuclein mutants and SUVs of POPG were kept constant in DBPS buffer, as 50  $\mu M$  and 2 mM respectively. Cuvette (Hellma) of pathlength 10 mm x 2mm was used. Tryptophan decay was collected in the presence and in the absence of  $\alpha$ -synuclein variants at 520 nm. The intensity decay were collected and analyzed.



## 2.9 AEDANS fluorescence anisotropy decay:

Time-resolved anisotropy decay measurements of the samples were made using a time-correlated single-photon-counting (TCSPC) setup (Fluorocube; Horiba Jobin-Yvon, NJ). The samples were excited using a 375 nm laser-diode (LD). The instrument response function (IRF) at 375 nm was collected using a aqueous solution of 2 % Ludox. The width of the IRF was ~ 200 ps. For the anisotropy decay measurements, the emission data were collected at 0 and 90 with respect to excitation polarization. The emission monochromator was fixed at 520 nm with a bandpass of 20 nm. The anisotropy decays were analyzed by globally fitting  $I_{||}$  and  $I_{\perp}$  as follows:

$$I_{||} = I(t)[1+2r(t)]/3 \quad (3)$$

$$I_{\perp} = I(t)[1-r(t)]/3 \quad (4)$$

The perpendicular component of the fluorescence decay was corrected for the G-factor of the spectrometer.  $I(t)$  is the fluorescence intensity collected at the magic angle (54.7) at time  $t$ . the anisotropy decays were analyzed using a bi-exponential decay model describing fast and slow rotational correlation time as follows:

$$r(t) = r_0[\beta_{fast} \exp(-t/\varphi_{fast}) + \beta_{slow} \exp(-t/\varphi_{slow})] \quad (5)$$

where  $r_0$  is the intrinsic fluorescence anisotropy,  $\varphi_{fast}$  and  $\varphi_{slow}$  are the fast and slow rotational correlation times; and  $\beta_{fast}$  and  $\beta_{slow}$  are the amplitudes associated with fast and slow rotational time.

The global (slow) rotational correlation time ( $\varphi_{slow}$ ) is related to viscosity ( $\eta$ ) and molecular volume ( $V$ ) by the Stokes-Einstein relationship as follow:

$$\varphi_{slow} = \eta V/kT \quad (6)$$

$$V = 4/3\pi R_h^3 \quad (7)$$

where  $R_h$  is the hydrodynamic radius of the molecule.

## Chapter 2

### Results and Conclusion

#### 1. Results

##### 1.2 Membrane-induced $\alpha$ -helical structure conformation of $\alpha$ -synuclein:

To monitor the conformational transition from an intrinsically disordered state to a highly helical state upon binding to negatively charged lipids, CD spectroscopic studies were employed. This was already carried out by Neha Jain and Karishma Bhasne.<sup>29, 30</sup> CD was employed to assess the effects of the Cys mutations and to characterize membrane-induced secondary structural changes for all the mutants. In pH 7.4 buffer solution (10mM HEPES, 50mM NaCl), CD spectra for wild-type and Cys mutant shows a minimum near 200 nm that is consistent with random coil configurations (Figure 2(a)). The CD spectra for the Cys mutant were not showing any secondary structural changes compare to wild-type protein, indicating that this change in amino acid does not change the native structure of protein.

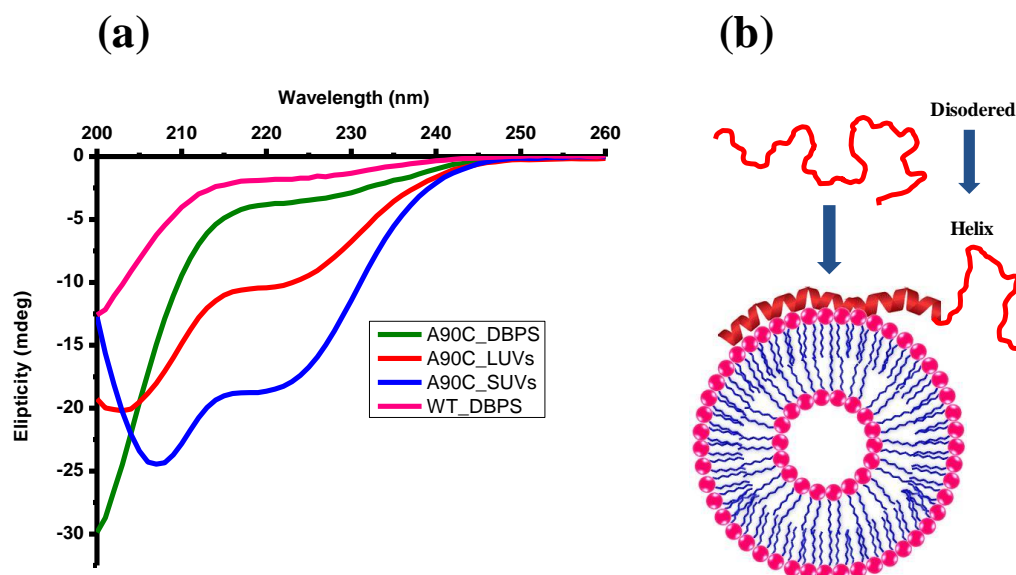


**Figure 2.** CD spectra of  $\alpha$ -synuclein. (a) CD spectra of wild-type (WT) (Pink) and cysteine mutant (Green) and Change in secondary structure from random coil (Green: Native) to  $\alpha$ -helix with SUVs (Blue) and LUVs (Red) (b) Schematic diagram to show the transition from disorder form to helical state.

In the presence of anionic phospholipids vesicles (SUVs & LUVs derived from POPG), we observed a transition from random coil state to a highly helical state upon binding with membrane (Figure 2(b)). We have chosen POPG SUVs & LUVs, since it is known to bind to  $\alpha$ -synuclein with higher affinity.<sup>29,30</sup> This preliminary result prompted us to understand this conformational change in residue specific manner.

## 1.2 Site-specific conformational dynamics of membrane-bound $\alpha$ -synuclein:

Site-specific interactions of alpha-synuclein with phospholipid vesicles were monitored by measuring steady-state and time-resolved AEDANS fluorescence anisotropy. The above results from CD and previous time-resolved Trp fluorescence studies from the lab done by Neha Jain lead us to perform further experiments to understand the residue specific conformational dynamics of  $\alpha$ -synuclein in membrane-bound state using long lifetime fluorescence probe IAEDANS.

Non-occurrence of cysteine in  $\alpha$ -synuclein gives us an advantage. So, 6 single-Cys mutants were generated over the polypeptide chain length (done by Karshima). For incorporating Cys, the residue positions at 9, 18, 56, 78, 90 and 140 were chosen based on earlier reports.<sup>32</sup> Steady-state anisotropy was low ( $0.017 \pm 0.001$ ) for the Cys variants in the free form, which indicates the protein, exist in the disordered form. In the presence of lipids anisotropy was high ( $0.06 \pm 0.01$ ), which indicates that protein is bound to membrane.

We have carried out picoseconds time-resolved fluorescence anisotropy measurements that provide insights into the local and global rotational dynamics of proteins.<sup>33, 34</sup> Global dynamics is represented by a slow rotational correlation time ( $\phi_{\text{slow}}$ ) that is generally related to the size (hydrodynamic radius) of the protein (Eq. 5-7). In the unbound form,  $\alpha$ -synuclein showed two rotational correlation times. The fast rotational correlation time,  $\phi_1$  is 0.34 ns for A90C (Table 1) which represents the local dynamics of AEDANS, whereas  $\phi_2$  is 2.2 ns, indicates the segmental mobility which does not depend on the protein size, since the segmental conformation fluctuations depolarize the fluorescence much more rapidly than the global tumbling of the polypeptide chain. For the membrane bound variant of the protein, three rotational correlation times were observed. Rotational correlation time  $\phi_2$  and  $\phi_3$  indicates the timescale as was observed in the free form. The slowest rotational correlation time,  $\phi_1$  is 64 ns, indicates the translational and diffusion

motion of protein over the membrane. This result indicates that  $\alpha$ -synuclein is tightly bound to the membrane near 90<sup>th</sup> amino acid. However, experiments need to be repeated to get the correct rotational correlation time as chi-Square values are high. The anisotropy decay for A90C in the membrane-bound form did not completely depolarize in the timescale of AEDANS fluorescence. The tumbling of SUV-protein complex is much slower (on the  $\mu$ s timescale, estimated from the size of SUVs). Whereas, in the unbound form, anisotropy of AEDANS decayed to zero indicating fast tumbling of protein (Figure 3).

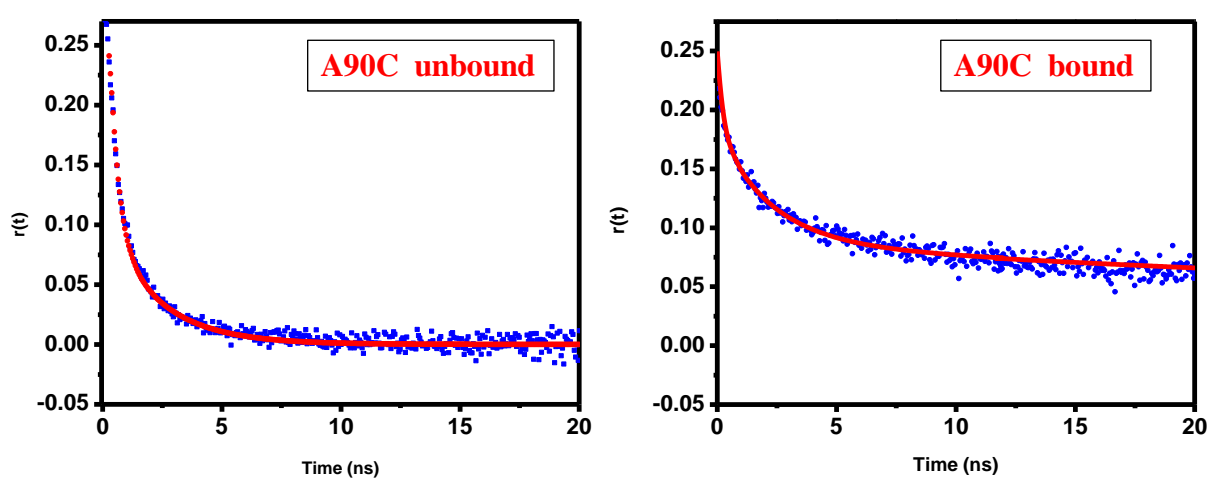


**Figure 3.** Picosecond time-resolved fluorescence anisotropy decays  $r(t)$  in the absence and presence of POPG SUVs of A90C. The solid line (Red) is the bi-exponential fit and tri-exponential fit respectively.

**Table 1.** IAEDANS fluorescence lifetime and rotational correlation time for single-Cys mutant of  $\alpha$ -synuclein (A90C) in the absence and presence of lipid membranes.

Cys Variants (Condition)	Fluorescence Lifetime in ns (amplitude)		Mean Lifetime in (ns)	Chi square value	Rotational Correlation time in ns (amplitude)			Initial anisotropy	Steady state anisotropy	Chi square value
	$\tau_1$ ( $\alpha_1$ )	$\tau_2$ ( $\alpha_2$ )			$\tau_{av}$	$\chi^2$	$\Phi_1$ ( $\beta_1$ )			
A90C (without SUVs)	10.13 (0.28)	13.64 (0.72)	12.64	1.08	2.2 (0.31)	0.34 (0.69)	---	0.3	0.02	1.92
A90C with SUV's	10.13 (0.28)	13.64 (0.72)	12.64	1.08	64.1 (0.3)	2.25 (0.3)	0.23 (0.4)	0.36	0.091	2.3

### 1.3 GdmCl-induced unfolding of Human $\beta_2$ -microglobulin:

Tryptophan (Trp) fluorescence is highly sensitive to its local environment, and thus often used as a reporter group for protein conformational changes. As surrounding polarity increases, the emission maximum shifts to the lower energy side because of the lowering of the energy level of the fluorescence emission state by stronger dipole–dipole interactions.<sup>33</sup> This fluorescence property is a useful indicator for the conformational change in proteins.  $\beta_2m$  contains two Trp residues at position 60 (exposed) and 95 (partially buried) (Figure 4(b)).<sup>26</sup> We first investigate the changes in intrinsic Trp fluorescence of  $\beta_2m$  from the native to a GdmCl-induced unfolded state. Under the native condition, Trp (W60) fluorescence showed a peak at 350 nm that corresponds to fully exposed tryptophan. As the GdmCl concentration increases to 1 M, there was a decrease in Trp fluorescence intensity, whereas, no shift in the  $\lambda_{max}$  was observed (Figure 4(c)). Further increase in GdmCl concentration till 2 M showed a blue shift in emission maximum which suggest that there are structural changes in  $\beta_2m$  at 60<sup>th</sup> position while unfolding. This region is getting buried in unfolding process and again getting exposed to aqueous environment at higher concentrations of GdmCl. The fluorescence intensity was reduced further and the maximum wavelength shifted to 345 nm.

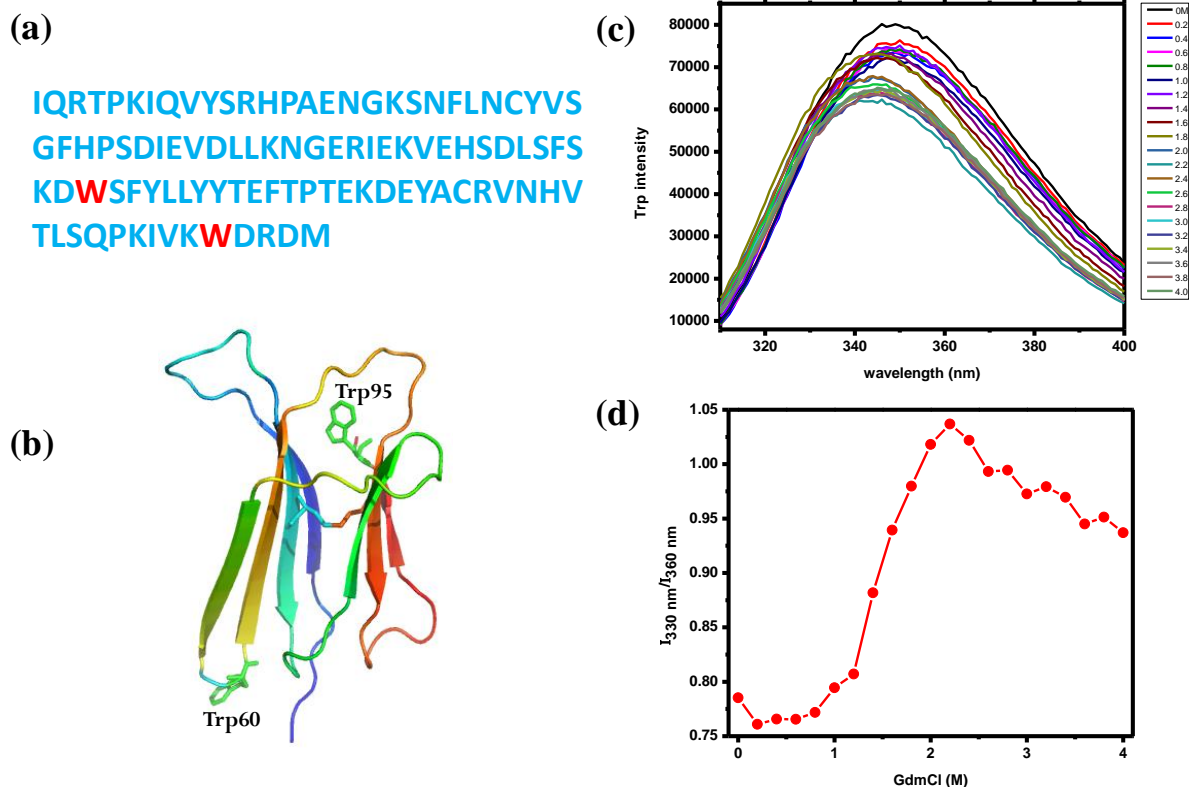


**Figure 4.**(a) Sequence of  $\beta_2m$  (b) Ribbon diagram of  $\beta_2m$  generating using PyMol (Delano Scientific LLC, CA) from the Protein Data Bank (PDB ID: 1LDS). (c) Fluorescence emission spectra of  $\beta_2m$  (W60) as function of increasing concentration of GdmCl (d) intensity ratios at 330nm and 360nm of  $\beta_2m$  (W60) as a function of increasing concentration of GdmCl.

#### 1.4 Thionitrobenzoate (TNB) quenches the fluorescence of tryptophan in a distance-dependent manner upon unfolding:

The absorbance spectrum of thionitrobenzoate (TNB) overlaps with the emission spectrum of tryptophan (Trp) (forming a FRET pair), and this has been used to measure distance changes during conformational transitions of proteins.<sup>35</sup>  $\beta_2m$  has two tryptophan residues located in two different positions- 60<sup>th</sup> & 95<sup>th</sup>. In this study, Trp residue at 60<sup>th</sup> position (W60) served as the fluorescence donor (D) and a TNB adduct attached via a thiol of an engineered single cysteine variant at N-terminal (W60 NTC-TNB) served as the FRET acceptor (A) (Figure 5 (a)). The fluorescence of Trp is quenched dramatically in the native state of W60 NTC-TNB and is also quenched to a lesser extent in the corresponding unfolded state (Figure 5 (b) & (c)) The observation that the extent of quenching of Trp fluorescence depends on the position of TNB in the protein, indicates that the quenching is distance-dependent.

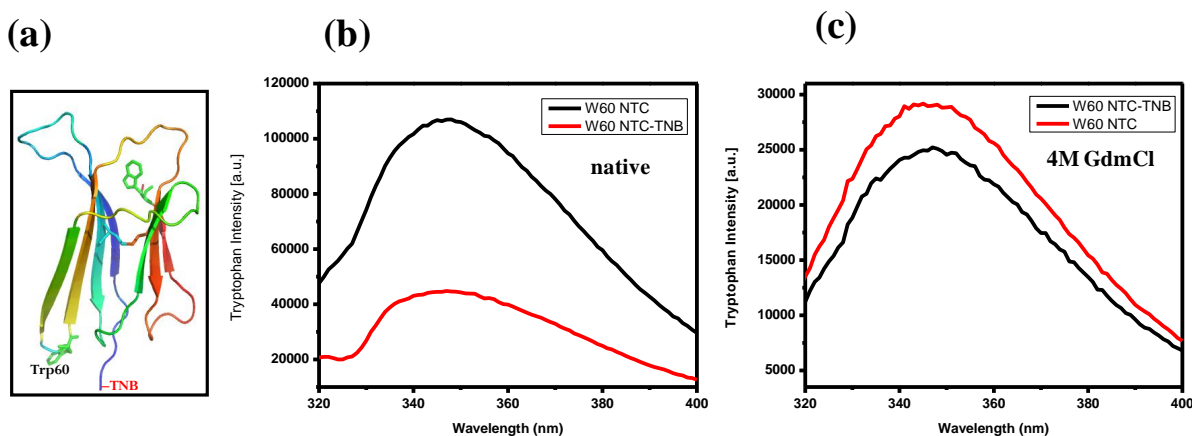


**Figure 5.** (a) Structure of  $\beta_2m$  the location of W60 and cysteine shown along with the TNB. The sole thiol moiety was labelled with TNB that quenches the fluorescence of Trp in a distance-dependent manner. The TNB-labelled protein named as W60 NTC-TNB. Structure was drawn from PDB file by using the program PyMOL. (b) Fluorescence emission spectra of unlabelled and TNB-labelled protein in native condition. (c) Fluorescence emission spectra of unlabelled and TNB-labelled protein in 4 M GdmCl.

To monitor the GdmCl-induced unfolding using FRET, the changes in the fluorescence of the donor alone ( $F_D$ ) and donor- acceptor ( $F_{DA}$ ) proteins were compared (Eq. 2). Figure 6 show the equilibrium unfolding transitions of the unlabelled and TNB-labelled proteins as monitored by change in FRET efficiencies. The fluorescence intensity increases during the unfolding reaction because the D-A distance is expected to increase as the protein unfolds. Hence, FRET efficiencies decreases with an increase in GdmCl concentration and showed mid-point of transition  $C_m$  1.19 M (Figure 6). Previous studies from the lab (done by Dominic Narang), we observed the  $C_m$  1.9 from far-UV CD data and fluorescence emission of  $\beta_2m$  W95. These differences in the  $C_m$  values and steady-state fluorescence studies consistently demonstrate the possibility of an intermediate whose conformation is different from the native and unfolded state during the unfolding process.

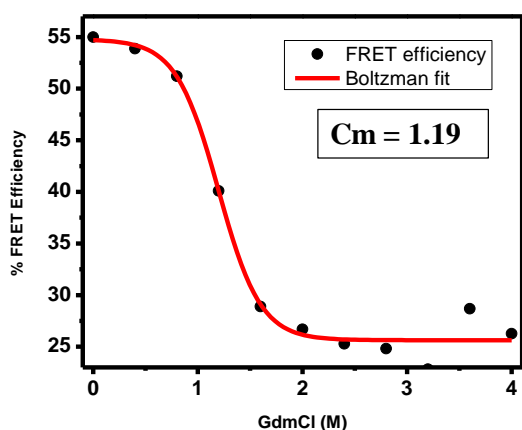


**Figure 6.** FRET efficiency is plotted against GdmCl concentration. The data for unlabelled and TNB-labelled protein is collected at the emission wavelength of 350 nm after excitation at 295 nm. The red continuous line through the data represent the Boltzmann fits to a two-state native  $\leftrightarrow$  unfolded model.

## **2.2 Conclusion and Future outlooks:**

This work presents structural and dynamical insights into the two amyloidogenic proteins.  $\alpha$ -synuclein adopts a  $\alpha$ -helical structure when it binds to lipid membranes. However the high resolution structural and dynamical insight of the membrane bound structure of  $\alpha$ -synuclein was not fully understood. Our result showed the different degrees of conformational organization of  $\alpha$ -synuclein upon binding to membranes. Further region-specific binding and folding studies of  $\alpha$ -synuclein to the membrane surface can elucidate the conformational dynamics of  $\alpha$ -synuclein. Additionally, this work also highlights the importance of studying a well-characterized model amyloid-forming protein using fluorescence methods to discern the conformational changes during GdmCl-induced unfolding. A variety of different fluorescence techniques have contributed to these findings, demonstrating the importance of fluorescent methods in the study of amyloidogenesis and membrane interactions. We believe that a combination of fluorescence techniques will be extremely useful to delineate the structural and dynamical signatures of amyloidogenic proteins.



## Bibliography

1. Luheshi LM, Crowther DC, Dobson CM (2008) Protein misfolding and disease: from the test tube to the organism. *Curr Opin Chem Biol* 12:25-31
2. Eichner T, Radford SE (2011) A diversity of assembly mechanisms of a generic amyloid fold. *Mol Cell* 43:8-18
3. Moreno-Gonzalez I, Soto C (2011) Misfolded protein aggregates: mechanisms, structures and potential for disease transmission. *Semin Cell Dev Biol* 22:482-487
4. Eisenberg D, Jucker M (2012) the amyloid state of proteins in human diseases. *Cell* 148:1188-1203
5. Uversky VN, Fink AL (2004) Conformational constraints for amyloid formation: the importance of being unfolded. *Biochim Biophys Acta* 1698:131–153.
6. Uversky VN (2009) Intrinsically disordered proteins and their environment effects of strong denaturants, temperature, pH, counter ions, membranes, binding partners, osmolytes, and macromolecular crowding. *Pro J* 28:305–326.
7. Crick SL, Jayaraman M, Frieden C, Wetzel R, Pappu RV (2006) Fluorescence correlation spectroscopy shows that monomeric polyglutamine molecules form collapsed structures in aqueous solutions. *PNAS USA* 103:16764-16769.
8. Mukhopadhyay S, Krishnan R, Lemke EA, Lindquist S, Deniz AA (2007) A natively unfolded yeast prion monomer adopts an ensemble of collapsed and rapidly fluctuating structures. *Proc Natl Acad Sci USA* 104:2649–2654.
9. Drescher M, Huber M, Subramaniam V (2012) Hunting the chameleon: structural conformations of the intrinsically disordered protein  $\alpha$ -synuclein. *Chem BioChem* 13:761–768.
10. Jain N, Bhattacharya M, Mukhopadhyay S (2011) Chain collapse of an amyloidogenic intrinsically disordered protein. *Biophys J* 101:1720–1729.
11. Trexler AJ, Rhoades E (2010) Single molecule characterization of  $\alpha$ -synuclein in aggregation-prone states. *Biophys J* 99:3048–3055.
12. Yamin G, Munishkina LA, karymov MA, Lyubchenko YL, Uversky VN, et al. (2005) Forcing nonamyloidogenic beta-synuclein to fibrillate. *Biochemistry* 44:9096-9107.
13. Yamamoto S, Hasegawa K, Yamaguchi I, Tsutsumi S, Kardos J, et al. (2004) Low concentrations of sodium dodecyl sulphate induce the extension of  $\beta_2$ -microglobulin-related amyloid fibrils at a neutral pH. *Biochemistry* 43:11075-11082

14. Rhoades E, Ramlall T.F, Webb W.W, Eliezere D, (2006) Quantification of  $\alpha$ -synuclein binding to lipid vesicles using fluorescence correlation spectroscopy. *Biophys. J.* 90:4692-4700.
15. Weinreb PH, Zhen W, Poon AW, Conway KA, Lansbury PT, Jr, (1996) NACP, a protein implicated in Alzheimer's disease and learning, is natively unfolded. *Biochemistry* 35:13709-13715.
16. Tamamizu-Kato S, et al. (2006) Calcium-triggered membrane interaction of the  $\alpha$ -synuclein acidic tail. *Biochemistry* 45:10947-10956.
17. Abeliovich A (2000) Mice lacking  $\alpha$ -synuclein display functional deficits in the nigrostriatal dopamine system. *Neuron* 25:239-252.
18. Cooper AA et al. (2006)  $\alpha$ -Synuclein blocks ER-Golgi traffic and Rab1 rescues neuron loss in Parkinson's models. *Science* 313:324-328.
19. Watson JB (2009) Alterations in corticostriatal synaptic plasticity in mice over-expressing human  $\alpha$ -synuclein neuroscience. *Neurosci.* 159:501-513.
20. J.M. George, H. Jin, W.S. Woods, D.F. Clayton, (1995) Characterization of a novel protein regulated during the critical period for song learning in the zebra finch. *Neuron* 15:361-372.
21. P.J. Kahle, M. Neumann, L Ozmen, V. Muller, H. Jacobsen, A. Schindzielorz, M. Okochi et al. (2000) Subcellular localization of wild-type and Parkinson's disease-associated mutant  $\alpha$ -synuclein in human and transgenic mouse brain. *J. Neurosci.* 20:6365-6373.
22. McLaurin J, Yip CM, St George-Hyslop P, Fraser PE (2000)  $\alpha$ -synuclein membrane interactions and lipid specificity. *J. Biol. Chem* 275:34328-34334.
23. Eliezer D, Kutluay E, Bussell R, Jr, Brown G (2001) Conformational properties of  $\alpha$ -synuclein in its free and lipid-associated states. *J. Mol. Biol.* 307:1061-1073
24. Gorevic PD, Munoz PC, Casey TT, DiRaimondo CR, Stone WJ, Prelli FC, Rodrigues MM, Poulik MD, Frangione B (1986) Polymerization of intact  $\beta_2$ -microglobulin in tissue causes amyloidosis in patients on chronic hemodialysis. *Proc Natl Acad Sci USA* 83:7908-7912.
25. Saper MA, Bjorkman PJ, Wiley DC (1991) Refined structure of the human histocompatibility antigen HLA-A2 at 2.6 Å resolution. *J Mol Biol* 219:277-319.

26. Trinh CH, Smith DP, Kalverda AP, Phillips SE, Radford SE (2002) Crystal structure of monomeric human  $\beta_2$ -microglobulin reveals clues to its amyloidogenic properties. *Proc Natl Acad Sci USA* 99:9771–9776.
27. Skora L, Becker S, Zweckstetter M (2010) Molten globule precursor states are conformationally correlated to amyloid fibrils of human  $\beta_2$ -microglobulin. *J Am Chem Soc* 132:9223–9225.
28. McParland VJ, Kad NM, Kalverda AP, Brown A, Kirwin-Jones P, Hunter MG, Sunde M, Radford SE (2000) Partially unfolded states of  $\beta_2$ -microglobulin and amyloid formation in vitro. *Biochemistry* 39:8735–8746.
29. Neha Jain (2013) PhD Thesis
30. Karishma Bhasne (2013) MS Thesis.
31. Wang GF, Li C, Pielak GJ (2010) 19F NMR studies of  $\alpha$ -synuclein-membrane interactions. *Prot. Sci.*19:1686-1691.
32. Shvadchak VV, Falomir-lockhart LJ, Yushchenko DA, Jovin TM, (2011) Specificity and kinetics of  $\alpha$ -synuclein binding to model membranes determined with fluorescent excited state intramolecular proton transfer (ESIPT) probe. *J Biol Chem* 286:13023-13032
33. Lakowicz, J. R. 2006. *Principles of Fluorescence Spectroscopy*, 3rd ed. Springer, New York.
34. Saxena A, Udgaonkar JB, Krishnamoorthy G. (2005). Protein dynamics and protein folding dynamics revealed by time-resolved fluorescence. In *Fluorescence Spectroscopy in Biology. Advanced Methods and their Applications to Membranes, Proteins, DNA*.
35. Jha SK, Udgaonkar JB (2009) Direct evidence for a dry molten globule intermediate during the unfolding of a small protein. *PNAS USA* 106(30):12289-12294.